Longitudinal critically refracted wave for residual stress assessment on a welded plate using 3D laser vibrometry

S.E. Salah Eddine Hebaz, F. Agon, Aziz Bouzzit, H. Walaszek, R. Hodé, F. Zhang, Stephane Serfaty, N. Wilkie-Chancellier

DOI: 10.61782/fa.2023.1009

forum acusticum 2023

LONGITUDINAL CRITICALLY REFRACTED WAVE FOR RESIDUAL STRESS ASSESSMENT ON A WELDED PLATE USING 3D LASER VIBROMETRY

S-E. Hebaz[1*] **F. Agon**[1] **A. Bouzzit**[1] **H. Walaszek**[2]
R. Hodé[2] **F. Zhang**[2] **S. Serfaty**[1] **N. Wilkie-Chancellier**[1]

[1] Laboratoire des Systèmes et Applications des Technologies de l'Information et de l'Énergie (SATIE), UMR CNRS 8029, CY Cergy Paris Université, F-95031 Neuville-sur-Oise, France

[2] Centre Technique des Industries Mécaniques, 52 Avenue Félix - Louat - CS 80067, 60304 Senlis, France

ABSTRACT

Local residual stresses, remaining in a material without any external load, generally result from manufacturing processes and associated deformations. Their characterization is important, as they can weaken the mechanical performance of the structure. Previous works have shown that ultrasonic techniques using longitudinal critically refracted waves (LCR) are successful for residual stress assessment near the surface in welded joints. In order to optimize the residual stress measurement, this work proposes a 3D scanning laser vibrometric detection, allowing to measure the three components of the displacement field produced by a LCR transducer over relatively long distances and on curved surfaces. The experiments are conducted for validation on a welded plate sample for which the calibration results are available in the literature. The base metal (BM) is P460 fine grain steel and the welding (Melted Zone) is performed along an X-shaped groove using the same filler metal. The wave generation is achieved by an angle beam piezoelectric transducer placed on the edge of the rectified area. Post-processing of vibrational signals acquired on the sample surface enables to extract the LCR wave and to construct the residual stress profile across the weld line. The results are in good agreement with those from the literature.

Keywords: *residual stress, LCR wave, 3D vibrometer, welded plates.*

[*] ***Corresponding author***: *Salah-eddine.hebaz@cyu.fr*

1. INTRODUCTION

Residual stresses (RS) refer to localized stresses that remain in a material without any external excitation. In some cases, they are intentionally induced to increase the strength of mechanical parts (e.g. heat treatment). In other cases, they are produced by manufacturing processes and associated deformations (machining, welding, rolling, etc.), and can negatively affect the performances of the structure and its service life. Therefore, their precise evaluation is essential to various industries [1].

Although they are distributed throughout the volume, their influence is mostly important on the surface. Accordingly, several techniques have been developed in the literature to evaluate compressive and tensile stresses in the outer layer of various mechanical components. On the one hand, one can find destructive (sectioning and slitting) and semi-destructive methods (micrographic analysis, extensometry, incremental hole-drilling). On the other hand, the current non-destructive testing (NDT) methods are either of limited application when the number of points to be examined is relatively large (X-ray diffraction, Neutron diffraction) or often reserved for simple geometries and require contact with the component (classical magnetic and ultrasonic methods). Detailed reviews of these methods and recent advances in SR assessment are provided in the following references [2-4].

However, many works have shown the potential of ultrasonic NDT methods using the longitudinal refracted wave at the critical angle (LCR) [4-6]. This sub-surface wave has the advantage of a non-dispersive propagation close to the surface, at a speed equal to that of the

longitudinal volume waves. This gives it a high sensitivity to residual stresses and internal defects near the interface, while being less affected by surface asperities [7].
Nevertheless, the measurement is most often based on the pitch-catch technique over short distances. The averaged variation of the LCR wave velocity is estimated between a transmitter and one or more piezoelectric receivers in direct contact with the part (via a polymethyl methacrylate wedge) or in local immersion (refraction at the water-steel interface). These classical techniques have limitations mainly related to the coupling quality and the characteristics of the transducers (dimensions, frequency, aperture, etc.). The latter influence considerably the characteristics of the LCR beam (formation, directivity and energy) [8]. The quality and repeatability of the measurement are thus impacted. Furthermore, the characteristics of the measuring devices limit the applicability of the technique to simple geometries and flat contact surfaces, and thus the scope of possibility in industrial application.

Today, non-contact NDT methods, especially laser-based ultrasound, are gaining momentum in the industrial field [3]. The application of these methods to the measurement of residual stress by LCR wave would have the advantage of greater flexibility, allowing the control of parts at a distance, and improving the spatial resolution and thus the accuracy of the measurement. It would also allow the measurement on complex geometries with small bending radii.
In this work, we are interested in the evaluation of near surface residual stresses in a welded metal plate using a 3D scanning laser vibrometer. It allows access to the three components of the displacement field. The aim is to optimize the detection of the LCR wave and its exploitation for the measurement of residual stresses. The experiments are conducted on a sample for which characterization results are available in the literature [5]. They are performed in two steps. First, the classical method is implemented with an immersion piezoelectric measuring device. The objective is to ensure the reproducibility of the measurement on the sample and to provide a basis to validate our approach. This will also allow us to identify areas of improvement in the processing of waveforms. The generation of the wave is performed by a piezoelectric compression transducer placed at the surface, with a wedge close to the critical angle.

This paper is organized as follows. In section (II), the theoretical aspects related to the generation of the LCR wave as well as the principle of the residual stress assessment method are presented. Section (III) shows the experimental validation results. Section (IV) presents the results of the laser vibrometer detection. Finally, a conclusion summarizing the main findings of this work is given in section (V).

2. MEASUREMENT METHOD

This section presents the refracted longitudinal wave and the principle of the measurement method, as well as its application to the estimation of residual stress in a weld.

2.1 Longitudinal critically refracted wave

The LCR wave is widely studied and used in the literature for residual stress assessment and near surface defect characterization [1-8]. It is a compressional wave that propagates in a solid below the interface (liquid-solid or solid-solid). It is generated at the first critical angle.

Consider on a plane reference frame (x_1, x_2) in which two media (1 and 2) are separated by a plane interface, as well as a longitudinal wave front in medium 1 incident at an angle θ_i on the boundary, as illustrated in Fig. 1. The direction of the transmitted waves depends on the properties of the 2nd medium. For an isotropic solid, the Snell-Descartes law is used to determine the angle of the refracted wavefronts in medium 2 [7]:

$$\frac{C_{l1}}{\sin\theta_i} = \frac{C_{l2}}{\sin\theta_{l2}} = \frac{C_{s2}}{\sin\theta_{s2}} \qquad (1)$$

with C_{l1} and C_{l2} the respective velocities of the longitudinal wave (L) in medium 1 and medium 2. C_{s2} is the velocity of the transverse wave (T) in medium 2. θ_{l2} and θ_{s2} are the refraction angles of the L and T wave respectively.

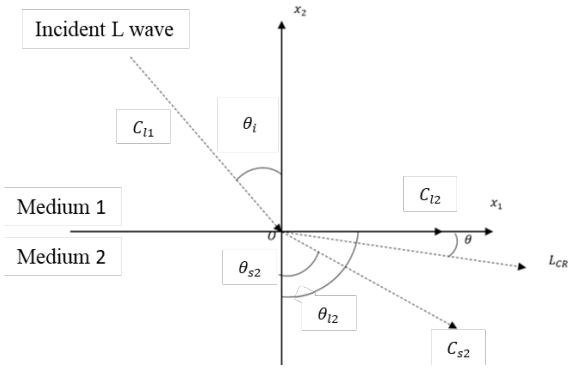

Figure 1. Generation of the LCR wave.

When the propagation velocity of the L-wave is higher in medium 2, there is an angle called the critical angle for which the transmitted L-wave does not propagate directly in the volume, but rather propagates in parallel to the interface, close to the surface of medium 2. We speak then of sub-

surface longitudinal wave, also called: longitudinal wave refracted at the critical angle or skimming wave. For isotropic media, this critical angle θ_c is obtained by:

$$\theta_c = sin^{-1}\left(\frac{C_{l1}}{C_{l2}}\right) \quad (2)$$

It propagates with a velocity equal to that of the longitudinal waves in the solid. The amplitude of the displacement is strongly attenuated compared to volume waves and decreases far from the source. However, it travels relatively long distances and retains a suitably high amplitude compared to evanescent waves. The displacement field distribution reveals a maximum amplitude at an angle of 10 to 20 degrees to the free surface [7,8]. Thus, the LCR wave has a sensitivity to defects and near-surface residual stresses present in the materials. Indeed, the residual stress affects its propagation velocity in a relatively significant way. Different studies have been conducted to compare the sensitivities of different types of waves to residual stresses. It has been shown that the LCR wave is the one with a significant potential for this type of application and show a relatively low sensitivity to surface roughness [9].

2.2 Acousto-elastic effect

The determination of residual stresses is based on the acousto-elastic effect. This effect is expressed by the change of the wave velocity according to the deformation of the solid. A formalism describing this phenomenon using the strain energy expression developed by Murnaghan [10] was presented by Hughes and Kelly [11]. The velocity variation is expressed as a function of the deformations generated by the applied or residual stresses, the elastic constants of the material and the Murnaghan elastic constants.
Consider a longitudinal wave propagating in direction 1, the propagation velocity is given by the following relation:

$$\rho_0 V_{11}^2 = C_1 + C_2\ trace(\varepsilon) + C_3\ \varepsilon_{11} \quad (3)$$

Where *trace(ε)* is the trace of the strain tensor. C_1, C_2 and C_3 are constants related to the material properties and the Murnaghan model. Considering an infinitesimal deformation and Hooke's linear law, the relation between the variation of the stress and the variation of the velocity (or that of the time of flight: $\Delta t = t - t_0$) can be established. In the case of a homogeneous material subjected to a uniaxial load along x_1, it can be expressed by the following simplified equation [5,6]:

$$\Delta\sigma_{11} = \frac{1}{K_{11}}\left(\frac{\Delta V_{11}}{V_{11}^0}\right) = -\frac{1}{K_{11}}\frac{\Delta t}{t_0} \quad (4)$$

where K_{11} represents the acousto-elastic coefficient, V_{11}^0 and t_0 are the velocity and time of flight in the stress-free material, respectively. This equation allows us to deduce the residual stresses when the constants t_0 (i.e. V_{11}^0) and K_{11} are known.

2.3 Measurement in a weld

In the case of a welded plate, it is necessary to determine the aforementioned constants in the base metal (BM) and in the melted zone (MZ) separately. The parameter t_0 is measured directly on the stress-free samples (or the unstressed area of the controlled part). The constant K_{11} is deduced experimentally from a uniaxial tensile test associated with an ultrasonic wave velocity measurement. The calibration curves of the samples are obtained during the loading and unloading phases without any hysteresis effect, so that the acousto-elasticity law can be established. The values on collected samples are obtained by:

$$K_{Zone} = -\frac{1}{\sigma}\frac{t - t_{0_{Zone}}}{t_{0_{Zone}}} \quad (5)$$

where σ is the applied stress, $t_{0\ Zone}$ the reference time of flight (at σ=0) in the studied zone. Finally, knowing the pair (K_{Zone}, $t_{0\ Zone}$) specific to each zone, the residual stress values are calculated from the following equation:

$$\sigma_{Zone} = -\frac{1}{K_{Zone}}\frac{t - t_{0_{Zone}}}{t_{0_{Zone}}} \quad (6)$$

It should be noted that the acousto-elastic coefficients must necessarily be determined for the controlled part because they are dependent on its microstructure. Especially since the latter is directly modified in the case of welding due to the high temperatures involved and the cooling kinetics. These variations must be taken into account in order to separate the effect of the stress from that of the microstructure, and thus improve the accuracy of the measurement [5,6].

3. EXPERIMENTAL VALIDATION

The first step in developing a new approach is to examin the existing method. This section presents a first measurement on a fully characterized sample using the conventional technique. The residual stress profile is estimated by an immersion piezoelectric measuring device.

3.1 Description of the sample and the measuring device

The sample studied here is a welded plate, already characterized in the work of J. Hoblos et al. [5]. It is of

length *L=330mm*, width *W=212mm* and thickness *H=30mm*. The BM is P460 fine-grained steel used for tanks, boilers and pipes, as it is temperature and pressure resistant. The welding is done following an X chamfer and using the same filler metal. The weld beam was flattened over an area of *Wr=100mm* for measurements. Fig. 2 shows the plate surface and its dimensions. The longitudinal wave velocity measurements in the two zones (BM and MZ) allowed to estimate the following values: $C_{l\ BM}$*=5928m/s* and $C_{l\ MZ}$*=5916m/s*.

(a)

(b)

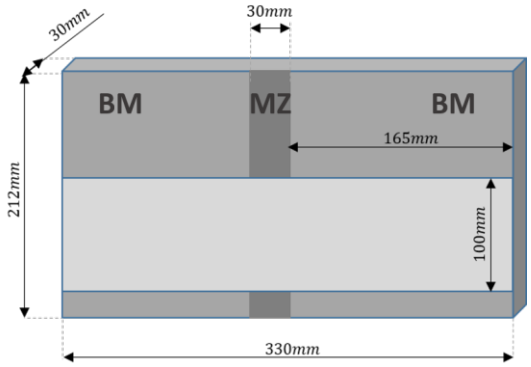

Figure 2. (a) Photo of the welded plate face and (b) drawing with its dimensions.

The measuring device consists of three cylindrical piezoelectric transducers: a transmitter (E) and two receivers (R1 and R2). They are wideband, single-element transducers with a central frequency f_c*=10MHz*, with a diameter of 0.250 inches, from KB AEROTECH®. The assembly is mounted on an aluminum block with an inclination (θ_{ic} *≈15°*) respecting the critical angle for immersion inspection of steel structures by LCR wave. Fig. 3 shows a picture of this device and a schematic of the transducer arrangement.

(a)

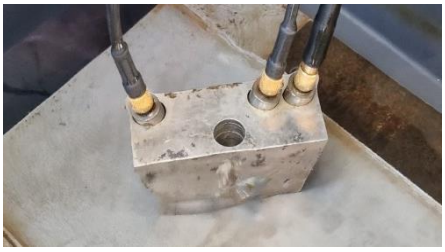

(b)

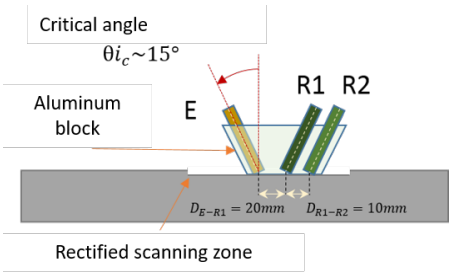

Figure 3. (a) Photo of the measuring device and (b) the corresponding diagram.

3.2 Experimental bench and measurement method

The experimental bench is composed of a Sofranel® DPR300 pulser/receiver, a Lecroy® Waverunner oscilloscope and an amplifier. The tests are conducted in Through transmission mode. The generator emits a negative pulse with an amplitude of about 300 volts to the transmitter E, with a repetition frequency *PRF=100Hz*. The receiver R1 is connected to the generator for amplification and filtering, then to the oscilloscope for viewing and recording time signals. The relative gain of the filter is fixed at 40dB for a bandwidth *BW=[1,15]MHz*. The R2 receiver is connected to the oscilloscope via an external amplifier. The test piece is immersed in a water bath and placed on two metal blocks. The transducer is positioned on the rectified surface of the plate. Fig. 4 shows a schematic of the setup.

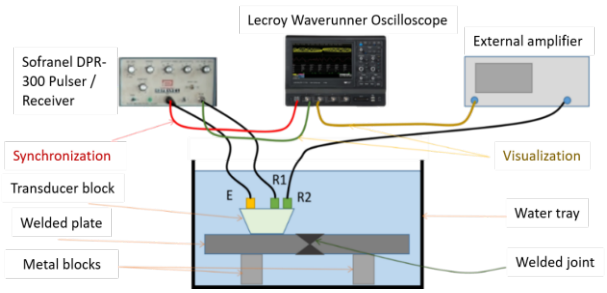

Figure 4. Setup of immersion ultrasonic testing for residual stress measurement.

The measurement performed consists of moving the transducer block along the rectified area from a position x_0, with a given step Δx. The scan direction is perpendicular to the propagation direction. Fig. 5 illustrates the scanning method. Since the distances $D_{E\text{-}R1}$ and $D_{R1\text{-}R2}$ are fixed (see Fig. 3-(b)), the estimation of the difference Δt in time of flight between the two receivers R1 and R2 depends only on the material properties, its microstructure and the residual stress in the propagation direction.

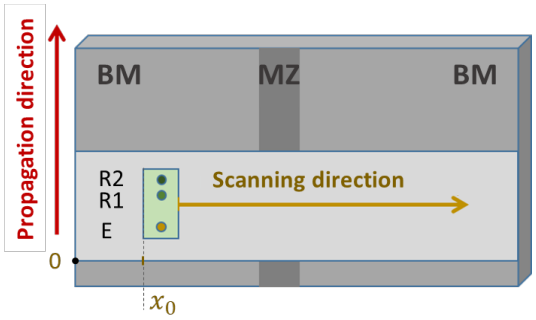

Figure 5. Diagram of the scan operated on the welded plate.

The knowledge of the pair (K, t_0) at each position is necessary to compensate the effect of the microstructure before inversion. The estimate of the residual stress is calculated using Eqn. (6). Thereafter, we consider only two acousto-elastic coefficient values corresponding to the BM and the MZ respectively, given in Tab. 1. These values were determined experimentally from a uniaxial tensile test associated with an ultrasonic measurement on stress-free samples taken from the welded plate [5]. To eliminate the stresses and keep the initial microstructure, they were heat treated below 600°C.

Table 1. Values of the acousto-elastic constants.

K_{BM}	K_{MZ}
$1.41e^{-5}MPa^{-1}$	$-1.69e^{-5}MPa^{-1}$

3.3 Results and discussion

The scan is performed over a length $L_{meas}=201mm$, with a spatial step $\Delta x=1mm$. The initial position is $x_0=50mm$ starting from the left edge of the plate. The signals from receivers R1 and R2 are recorded on the oscilloscope, averaged 100 times, with a sampling frequency $fs=2.5GHz$, and then transferred to the computer for post-processing.
Once the scan is completed, two matrices of the spatio-temporal signals, corresponding to the R1 and R2 receivers, are obtained. To extract the relevant information, a post-processing of the raw signals is performed. The algorithms are implemented on MATLAB ®. A digital filtering is performed using a bandpass filter of a bandwidth $BW=[f_c/2, 3f_c/2]$. Then, the LCR wave packet is extracted using a Kaiser-Bessel derivative window. The amplitude is normalized to the maximum to ensure good accuracy of the time-of-flight estimation. A smoothing is applied to the variation curve to eliminate measurement errors, aberrant peaks and trend. Finally, the residual stress profile is calculated using Eqn. (6). Fig. 6 shows the obtained results.

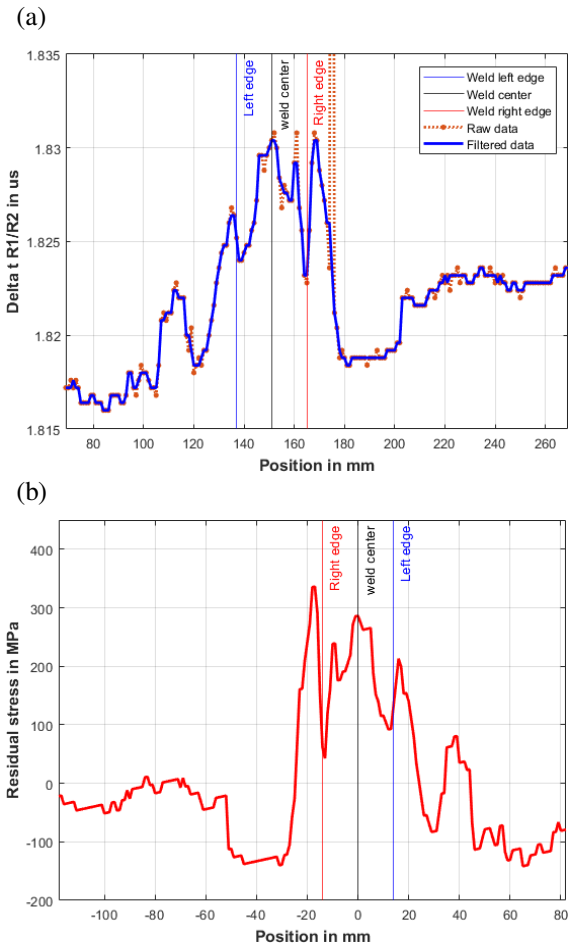

Figure 6. (a) Estimation of the time-of-flight variation across the weld and (b) the corresponding residual stress profile.

Fig. 6-(a) represents the variation of Δt as a function of position x_i across the weld. The vertical lines on the plot show the center and visible boundaries of the weld measured directly on the plate. Overall, these results show

an increase in the time of flight, implying a decrease in the propagation velocity throughout the weld area, which is consistent with velocity estimates in stress-free samples. Nevertheless, the full-scale Δt variation amplitude $\Delta t_{FS} \approx 16ns$ is much higher than the unstressed case (corresponding to the microstructure change), $\Delta t_{FS}^{0} \approx 3.42ns$. This indicates that the variation corresponds indeed to the residual stress. Furthermore, we can distinguish peaks and troughs near some significant positions, especially the one at the center and those at the edges of the weld. We also observe that the variation of Δt extends beyond the visible boundaries of the weld. Then, after about 100 mm from the center, the time-of-flight difference becomes virtually constant. Together, they define intervals that correspond, a priori, to the different zones commonly encountered in this type of weld: the melted zone, the heat-affected zone (HAZ), and the fusion zone.

Moreover, Fig. 6-(b) depicts the reconstructed residual stress as a function of position $X_i = (x_{wc} - x_i)$. The graph was horizontally shifted to the weld bead center position (x_{wc}) and reflected across the vertical axis, in order to facilitate the comparison. The obtained profile is in good agreement with those found in the literature [4-6] and they are in relatively of the same order of magnitude as those of J. Hoblos et al [5] (obtained for 2MHz and $\Delta x = 5mm$). On the one hand, the residual stress level (tensile) reaches a maximum of about 350MPa near the right edge of the weld and 300MPa at its center. On the other hand, it drops to a level (compressive stress) below -100MPa near the HAZ and then returns to around zero (unaffected base metal).

In fine, these results confirm a reproducibility of the measurement despite the difference in instrumentation, and scan parameters (frequency and spatial step). Also, they constitute a clear validation of the method and provide a basis to examine the 3D Laser vibrometer measurement.

4. MEASUREMENT BY 3D VIBROMETER

In this section, the detection is performed using the 3D laser scanning vibrometer. This will allow us to examine closely the potential of this type of instrumentation in the context of residual stress analysis by LCR wave.

4.1 Description of the experimental bench

In order to overcome the limitations of contact transducer measurements, the experiment is conducted using a full-field scanning laser vibrometer PSV-500-3D-V (*HeNe, Class II, P<1mW/cw, λ=632-680nm (red), f_{max}=25MHz*) from Polytec®. It allows access to the three components of the displacement field (U_x, U_y, U_z). The purpose is to evaluate these different components of the LCR wave at the solid surface in order to explore its exploitation for residual stress measurement.

Fig. 7 presents a synoptic of the experimental bench setup. It is composed of the JSR Ultrasonics® DPR300 pulse generator, the three laser heads of the PSV-I-500 positioned on a rigid table tripod (PSV-A-T34) and the associated control unit. The latter enables the configuration of the scan parameters, the recording and the pre-processing of the extracted time signals.

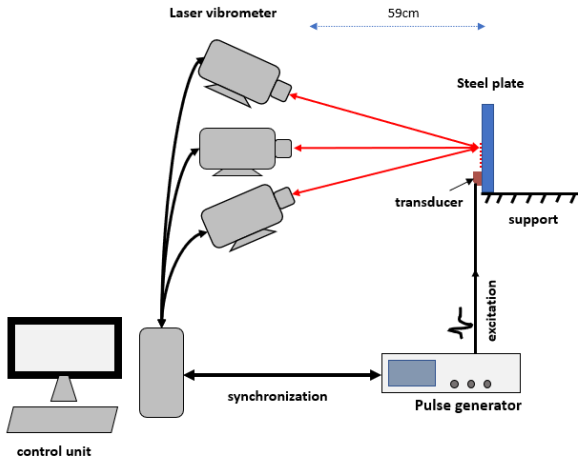

Figure 7. Diagram of the 3D scanning laser vibrometer experimental bench.

The welded plate is positioned on a support in front of the laser. An adhesive reflective tape is applied in the scan area for improve signal return. The emitter block is placed on the surface of the plate on the edge of the rectified area, as shown in Fig. 8. It consists of a compression angle beam piezoelectric transducer (Panametrics® C540-SM) of a center frequency $f_c = 10MHz$ and a diameter of about 13mm. It is mounted on a screw-in wedge (ABWM-5T-30) with a tilt angle of $\theta i = 25°$. The refraction of the longitudinal wave at this angle reaches the vicinity of the calculated critical angle ($\theta_c \approx 27°$) and thus the generation of the LCR wave. The coupling with the plate surface is ensured via a glycerine-based gel (Olympus® D12) suitable for longitudinal wave metal inspection.

The generator is set on Echo mode (T/R). It emits a negative spike pulse (~10-70ns typical full duration at half maximum) with an amplitude of about 475volts to the transmitter. The repetition rate is set to $PRF = 1kHz$. The laser scan is performed along the propagation direction corresponding to the axis of the emitter transducer wedge,

starting from a distance y_0=33mm (i.e. 2mm from the tip of the wedge). Time signals are extracted for a set of Ny=71 points with a spatial step Δy=0.5mm (this is the lower limit allowed by the laser). The transmitter is moved along the scanning area across the weld, over a length L_{meas}=250mm with a spatial step Δx=2mm. The starting position is x_0=30mm from the left edge of the plate. Fig. 8 illustrates the scan configuration, the transducer block position and the laser extraction points (red dotted line). The local coordinates system of the vibrometer is set as pictured.

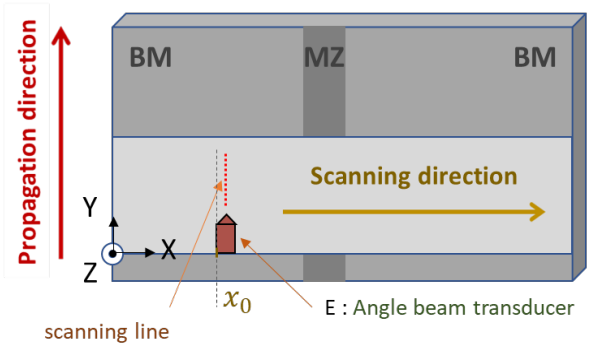

Figure 8. Scheme of the scan configuration.

The time signals are pre-processed and recorded via the laser controller, then transferred to the computer for post-processing. An averaging of 2048 is used per signal, with the maximum allowed sampling frequency f_s=62.5MHz. A fist filtering is applied using a high-pass filter with a cut-off frequency of 200kHz, to eliminate the low frequency components. After going through all the points of the spatial window, we obtain the matrices of the spatio-temporal signals. The same post-processing mentioned above is applied to extract the relevant information.

4.2 Results and discussion

The complete sweep has generated over 126×71×3 time signals of 1000 sample each. For practical reasons, we limit the analysis to those corresponding to the components U_y and U_z obtained in the region of interest: x=[124, 180] and the pair of detection points (y_3=34mm, y_{61}=63mm). Fig. 9 shows two examples of spatio-temporal representing tangential and normal displacements of the LCR wave.

The results confirm that the tangential component is most energetic one and thus potentially more advantageous for the intended application. Its maximum amplitude is almost three times that of the normal component, within the first few millimeters of propagation distance. However, a strong decay rate is observed between the detection points. This behavior is expected for a compressional wave with an axis of propagation oblique to the surface. But, it is accompanied by a high noise level, compared to U_z, which makes it very difficult to extract the time of flight variation with acceptable accuracy. Consequently, in this work, only the normal component signals will be used for the residual stress estimation.

(a)

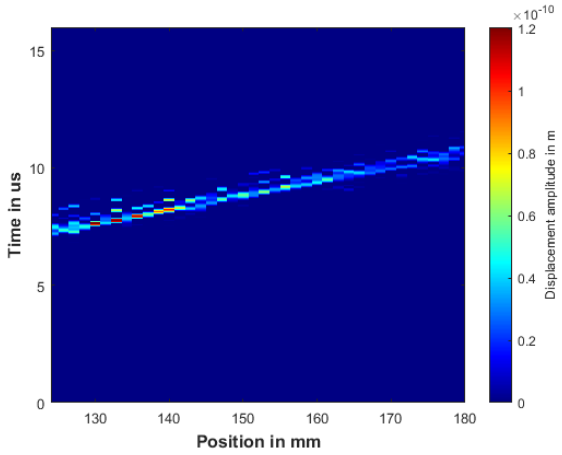

(b)

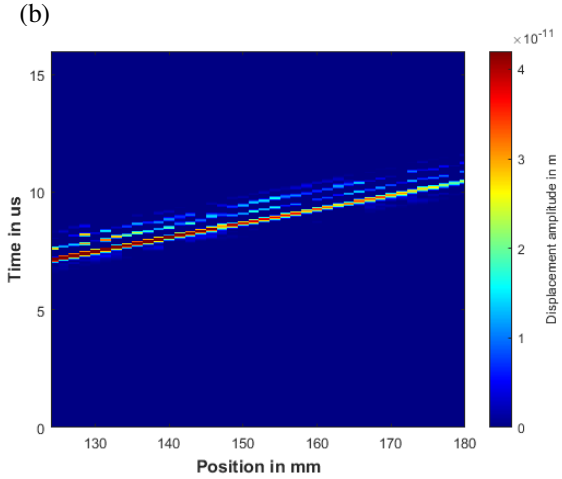

Figure 9. Spatio-Temporal signals: (a) tangential U_y and (b) normal displacement U_z.

Fig. 10 shows the time of flight variation between the LCR wave packets of the signals extracted from y_3 and y_{61}, as well as the corresponding residual stress profile. The results are roughly similar to those of the validation experiment (depicted in Fig. 6), despite the noise due to experimental conditions (adhesive reflective tape, low sampling frequency and spatial step, wedge tilt and attenuation, etc.). The tensile RS level reaches a maximum of about 440MPa at it center. The compressive RS is below 200MPa near the HAZ and goes back to zero.

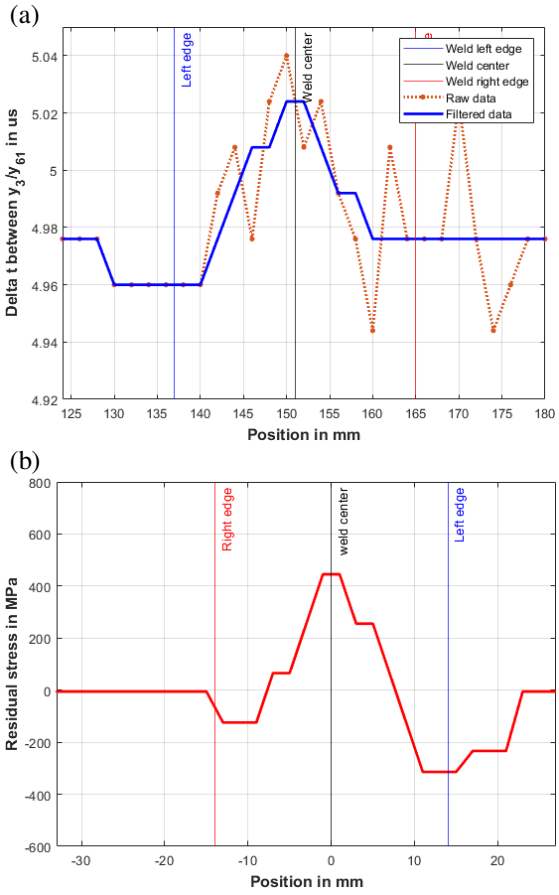

Figure 10. (a) Time-of-flight variation between y_3 and y_{61} and (b) the corresponding residual stress profile.

5. CONCLUSION

This study shows the potential of the LCR wave measurement using a full-field vibrometric solution to assess residual stress in metallic parts. The 3D vibration analysis allowed the measurement of normal and tangential components on the surface of the samples. The preliminary results showed that a profile similar to that of approved methods can be obtained. Moreover, the tangential component is found to be conceptually suitable for this type of application. If the signals are noisier than those of the normal one, they are still complementary and of interest for future work on this subject. It should allow to increase the accuracy of the time of flight estimation for a better evaluation of the residual stress. This is a promising line of work to develop a contactless control method for large complex-shaped parts. In other respects, the encountered problems can be overcome by means of a laser of power for excitation associated to an infrared laser detection.

6. ACKNOWLEDGMENTS

This work was carried out as a part of a research collaboration contract between the SATIE laboratory of CY Cergy Paris Université and the CETIM Senlis, France.

7. REFERENCES

[1] G. Totten, "*Handbook of residual stress and deformation of steel"*, ASM international, 2002.

[2] P. J. Withers et al. "Recent advances in residual stress measurement." *International Journal of Pressure Vessels and Piping* 85.3 (2008): 118-127.

[3] R. Acevedo et al. "Residual stress analysis of additive manufacturing of metallic parts using ultrasonic waves: State of the art review." *Journal of Materials Research and Technology* 9.4 (2020).

[4] M. Gel'atko et al. "Longitudinal critically refracted (LCR) ultrasonic wave for residual stress measurement." *IOP Conference Series: Materials Science and Engineering*. IOP Publishing, 2021.

[5] J. Hoblos et al., " Evaluation des contraintes résiduelles induites par soudage par la méthode ultrasonore : analyse de l'effet de la microstructure" , *Mécanique & Industries 8*, 27–33 (2007)

[6] H. Qozam et al., "Microstructure Effect on the Lcr Elastic Wave for Welding Residual Stress Measurement", *Experimental Mechanics* (2010).

[7] J. L. Rose, "*Ultrasonic waves in solid media*." Cambridge University Press, 2014.

[8] N. Pei et al., "Analysis of the directivity of Longitudinal Critically Refracted (LCR) waves", *Ultrasonics* 113 (2021) 106359.

[9] J. Hughes et al. "Comparative evaluation of in situ stress monitoring with Rayleigh waves." *Structural Health Monitoring* 18.1 (2019): 205-215.

[10] F. D. Murnaghan, "Finite deformations of an elastic solid", *American Journal of Mathematics*, 59(2):235-260. (1937)

[11] D. Hughes and J. Kelly, "Second-order elastic deformation of solids", *Physical Review* 5(92):1145–1149, 1953.